

Figure S1. Expression and subcellular localization of Dicer upon DNA damage in HEK 293 cells. (A and B) Immunoblots detecting total Dicer (A-2) and phosphorylated histone variant H2A.X (γH2A.X, S139) after continuous DNA damage (A) or pulse-chase treatment (B). Immunoblots were quantified using ImageJ. (C and D) Immunoblots detecting total (A-2) or phosphorylated (p-DCR-1) recombinant TAP-tagged Dicer after depletion of endogenous Dicer, reexpression of TAP-tagged Dicer, and immunoprecipitation from nondamaged (control) and damaged (H₂O₂) nuclear fractions. Immunoblots were quantified using ImageJ. #, nonspecific signal. (E) Confocal imaging of phosphorylated Dicer (p-DCR-1) and γH2A.X. (F) Confocal imaging of phosphorylated (p-DCR-1) and total (13D6) Dicer in wild-type and Dicer-depleted (Dicer KD) cells. (G) Confocal imaging of phosphorylated Dicer (p-DCR-1) in HEK293 cells. HU, hydroxyurea. (H) Immunoblots detecting total Dicer (A-2), phosphorylated ATM/ATR substrates and γH2A.X in HEK293 cells. α-Tubulin, loading control. (I) Real-time proliferation assay measuring the “cell index” as a function of impedance change over time. Arrowhead, addition of drugs; green box, time frame of analysis. (J) Immunoblots detecting Ki-67, cleaved Poly ADP-ribose polymerase (PARPc) and γH2A.X after drug treatment. H₂O₂, hydrogen peroxide; MMS, methyl methanesulfonate; STS, staurosporine; Gy, gray; IN, input; SN, supernatant; IP, immunoprecipitation; IB, immunoblot.

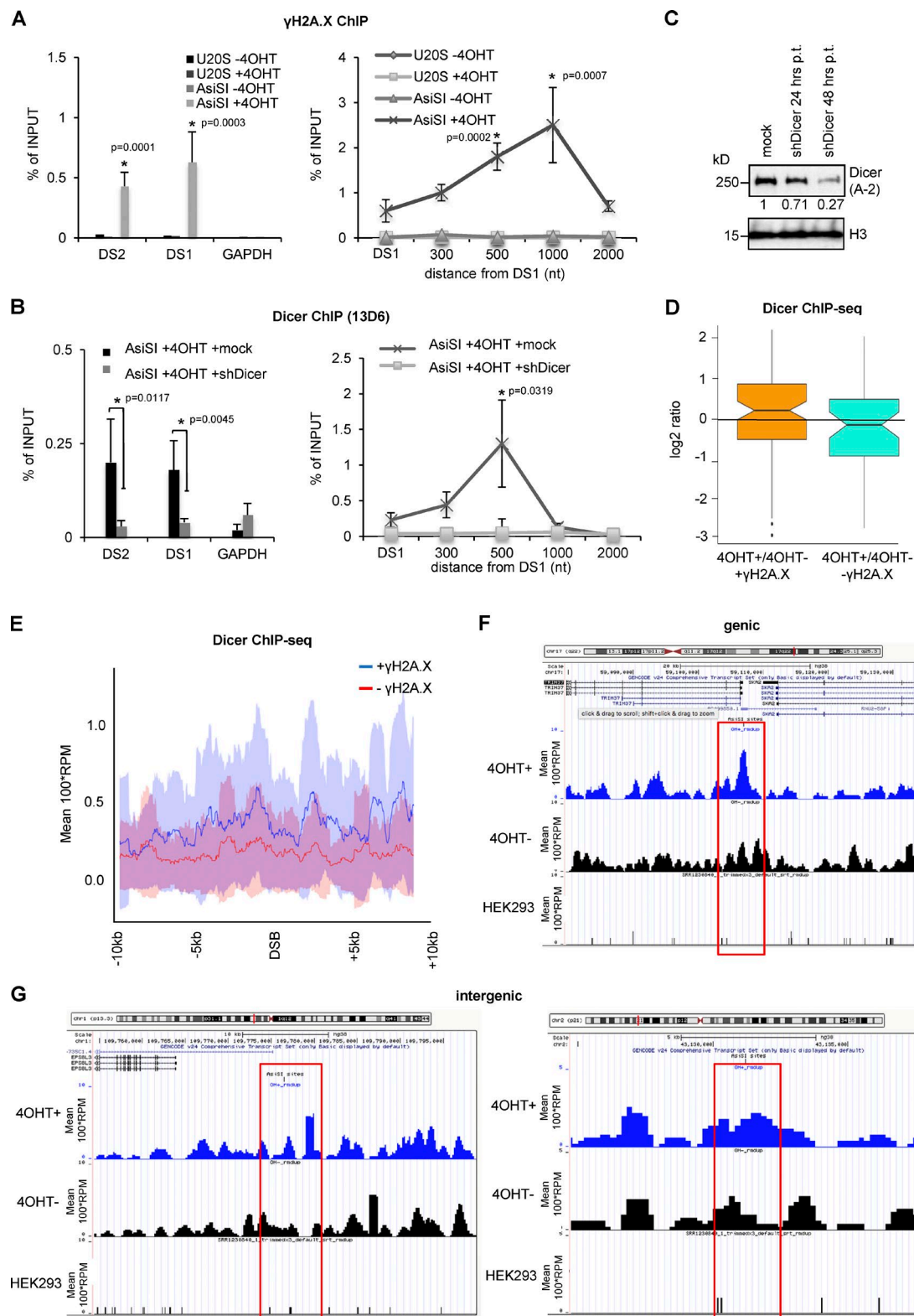


Figure S2. **Dicer occupancy at DNA double-strand breaks in AsiSI-ER U2OS cells.** (A and B) ChIP analysis showing γ H2A.X (A) and Dicer (B) occupancy at DSBs DS1/2 in wild-type and Dicer-depleted AsiSI-ER U2OS cells using site-specific primers. GAPDH, control locus. 4OHT, 4-hydroxytamoxifen; *, $P < 0.05$; error bars, means \pm SEM of three biological replicates. (C) Immunoblots detecting Dicer levels after transfection of Dicer-targeting shDicer. p.t., posttransfection. Control, mock-transfected cells. (D) Box plot showing levels of Dicer ChIP-seq in log₂ ratios of 4OHT+/4OHT- conditions for both, 99 γ H2A.X-positive and 99 γ H2A.X-negative sites in -500 bp/+500 bp around the AsiSI site window. Horizontal black line extends the y-axis 0 value for better visibility. Median value is indicated as a horizontal black line within the box plots. $P = 0.0551$, Wilcoxon rank-sum test. (E) ChIP-seq signal in HEK293 cells at γ H2A.X-positive AsiSI sites (top 200, blue) and genic γ H2A.X-negative AsiSI sites (bottom 200, red) after duplicate read removal. A rolling mean of 1 kb was applied after removal of 2% of the top and bottom values. Shadow, rolling SD. (F and G) Snapshots showing examples of Dicer binding at AsiSI target sites before (4OHT-) and after (4OHT+) DNA damage at genic and intergenic cut AsiSI sites. Red box, proximal region to AsiSI site.

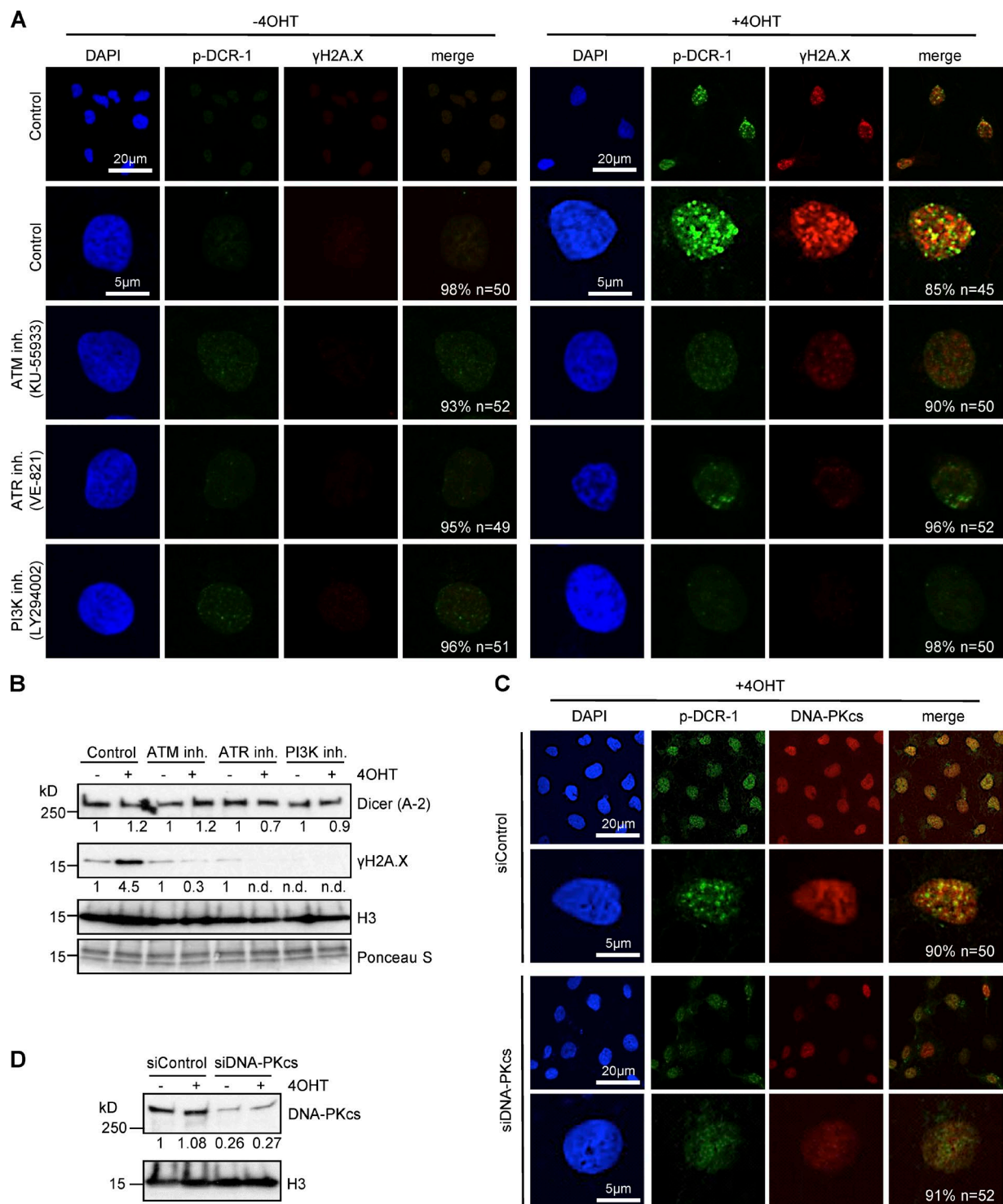


Figure S3. **Phosphorylation of Dicer by phosphatidylinositol-3-kinase (PI3K) signaling in AsiSI-ER U2OS cells.** (A) Confocal imaging of phosphorylated Dicer (p-DCR-1) and γ H2A.X after preincubation with kinase inhibitors. All quantifications represent the number of cells that exhibit the shown phenotype. (B) Immunoblots detecting γ H2A.X levels after preincubation with kinase inhibitors. n.d., not detectable. (C) Confocal imaging of phosphorylated Dicer (p-DCR-1) and γ H2A.X after depletion of DNA-dependent protein kinase, catalytic subunit (DNA-PKcs). All quantifications represent the number of cells that have the shown phenotype. In siDNA-PKcs cells, only cells with efficient depletion of DNA-PKcs were considered for quantification. (D) Immunoblots detecting DNA-PKcs after depletion of DNA-PKcs by siRNA.

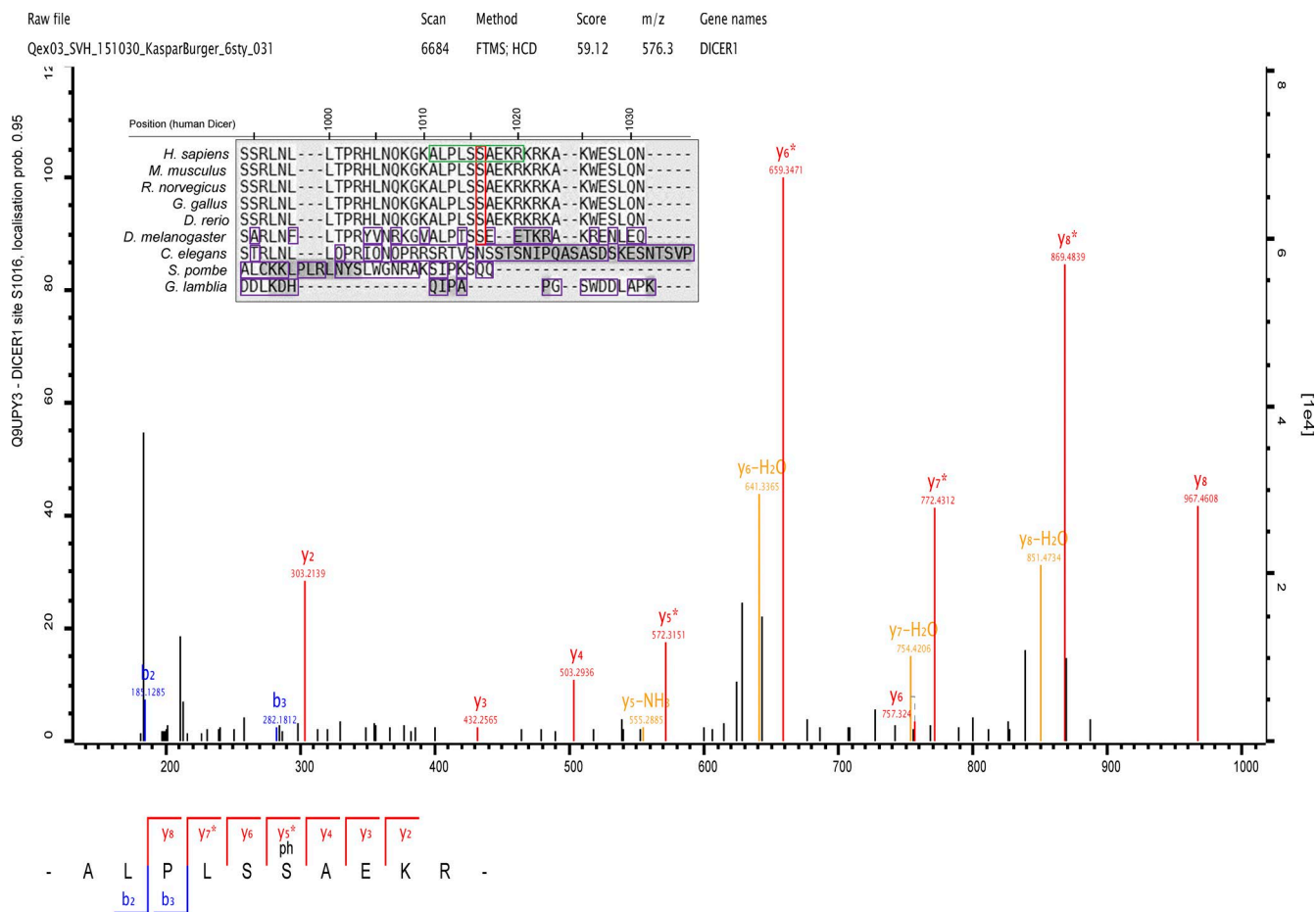


Figure S4. **Chromatogram of Dicer spectral counts for residue S1016 in HEK293 in cells.** Fragmentation spectra of ion series at Dicer residue S1016 in HEK293 cells. Box, alignment of the platform-PAZ-connector helix cassette aa sequence surrounding residue S1016 across species; green, damage-induced phosphopeptide; red, conserved S1016 residue; purple, nonconserved residues. Fragmentation spectra of individual phosphopeptides available on request.

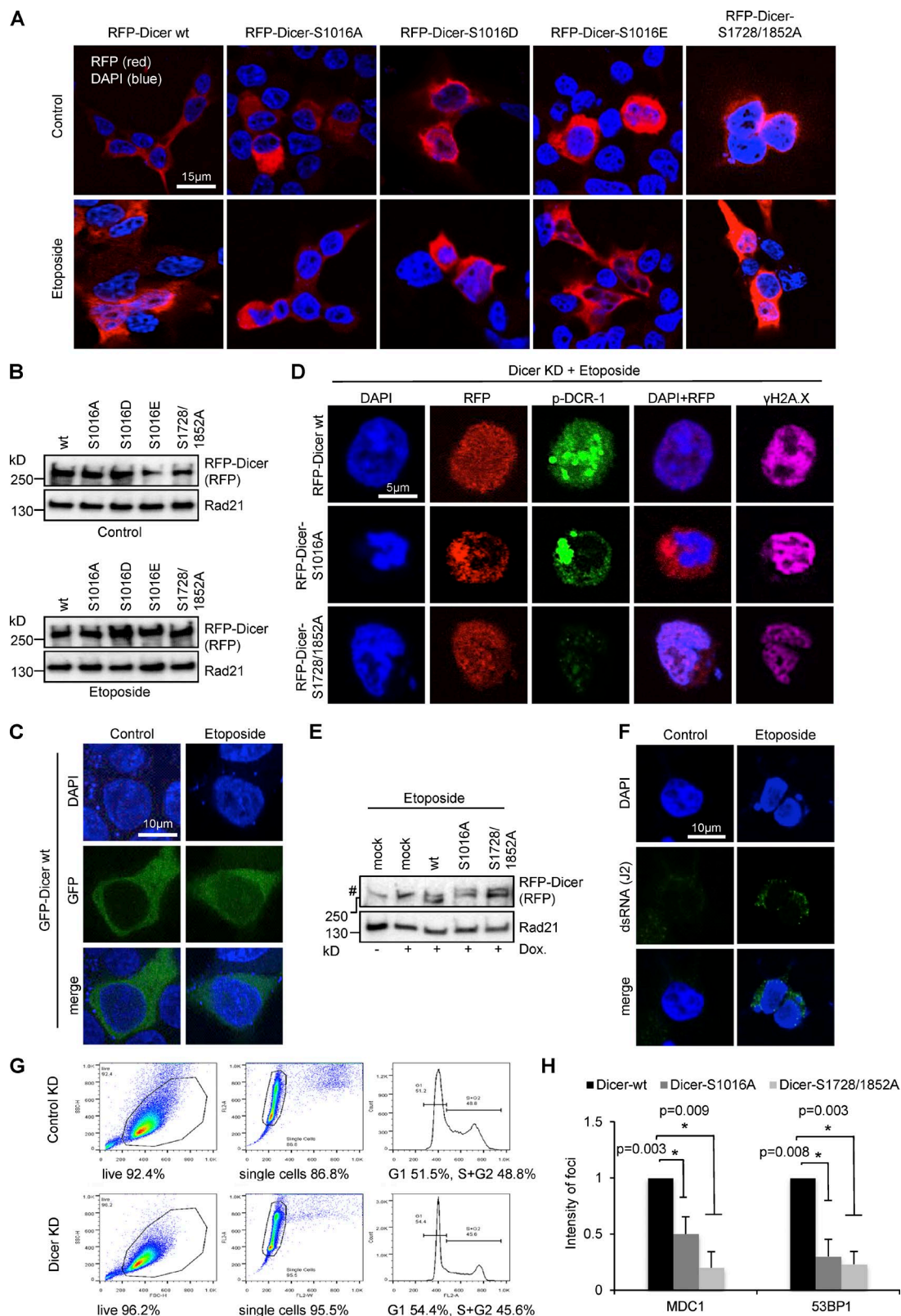


Figure S5. **Differential subcellular localization of RFP-Dicer mutants in HEK293 cells.** (A) Confocal imaging of RFP-Dicer constructs. Merged images are shown. (B) Immunoblots detecting expression of RFP-Dicer constructs. Rad21, loading control. (C) Confocal imaging of GFP-tagged wild-type Dicer, $n > 30$. (D) Confocal imaging of RFP-Dicer constructs, phosphorylated Dicer (p-DCR-1), and γ H2A.X in Dicer-depleted (Dicer KD) cells transfected with RFP-Dicer constructs, $n > 30$. (E) Immunoblots detecting expression of RFP-Dicer constructs in wild-type and Dicer-depleted (Dicer KD) cells. (F) Confocal imaging of dsRNA (J2), $n > 30$. (G) Flow cytometry analysis assessing the cell cycle distribution of Dicer KD cells. Control KD, induction of scrambled shRNA knock-down. Dox., doxycycline; Rad21, loading control; #, unspecific signal. (H) Quantification of MDC1 and 53BP1 foci per cell, as shown in Fig. 7 (E and F) in 4OHT+ 2 h condition. Error bars are derived from three biological repeats. At least 40 cells were counted per repeat. *, $P < 0.05$.

Table S1. Quantification of damage-induced nuclear Dicer phosphoresidue serine-1016

Dicer peptide sequence	Modification	Mass	PEP	Score	Intensity control	Intensity etoposide	Ratio Eto:Ctrl
ALPLSSAEKR	Phospho (STY)	1,150.575	0.004008	53.03	195,960	654,860	3.342
APKEEADYEDDFLEYDQEHIR	—	2,611.135	2.62 ⁻⁸	67.93	303,760	242,380	0.798
EAGKQDPELAYISSNFITGHGIGK	—	2,531.266	9.83 ⁻²⁰	92.79	3 ⁶	2,750,100	0.912
RSEEDKEEEDIEVPK	—	1,959.891	0.001267	41.54	249,080	282,200	1.133

PEP, posterior error probability.

Table S2. Nuclear Dicer phosphopeptides identified by mass spectrometry

Residue	Peptide
S1016	ALPLSpSAEKR
S1142	TSpSLENHDQMSVNCR
S1160	TLLSEpSPGK
S1250	pSTSDGSPVMAVMPGTTDTIQVLK
S1468	KlpSLSPFSTTDSAYEWK
S1470	ISlpSPFSTTDSAYEWK
S1868	ELLEMPEPETAkFpSPAER

Table S3. Primer pairs used for site-directed mutagenesis

Primer	Sequence (5'–3')
S1016A-forward	AAGCGCTGCTGAGAAGAGGAAAGCCAAATG
S1016A-reverse	CAGCAGCGCTTAAAGGAAGCGCTTTCCCC
S1016D-forward	AAGCGATGCTGAGAAGAGGAAAGCCAAATG
S1016D-reverse	CAGCATCGCTTAAAGGAAGCGCTTTCCCC
S1016E-forward	AAGCGAGGCTGAGAAGAGGAAAGCCAAATG
S1016E-reverse	CAGCCTCGCTTAAAGGAAGCGCTTTCCCC
S1728A-forward	GCACGCACCGGGGTCCTGACAGACCTGCGG
S1728A-reverse	CCGGTGCGTGCTGCCGCGGCTTTCATAAAG
S1852A-forward	CCGTGCACCTGTGCGAGAATTGCTTGAAATG
S1852A-reverse	CAGGTGCACGGGTACATTTGCAGAAAACCTT

Table S4. Primer pairs used for ChIP and quantitative RT-PCR analysis

Primer	Sequence (5'–3')
GAPDH-fwd (chromosome 12)	AACCTGCCAAATATGATGAC
GAPDH-rev (chromosome 12)	AGGAAATGAGCTTGACAAAG
DS2-fwd (chromosome 6)	TGCCGGTCTCCTAGAAGTTG
DS2-rev (chromosome 6)	GCGCTTGATTCCCTGAGT
DS1-fwd (chromosome 1)	GATTGGCTATGGGTGTGGAC
DS1-rev (chromosome 1)	CATCCTTGCAAACCACTCCT
300-fwd (chromosome 1)	AGGACTGGTTTGAAGGATG
300-rev (chromosome 1)	ACCCCATCTCAAATGACAA
500-fwd (chromosome 1)	CCTGGATATGAGTTTGATCAGC
500-rev (chromosome 1)	CTCTCCTTTGCTGACACTG
1000-fwd (chromosome 1)	AGGAATTGACTGCGGTGTTT
1000-rev (chromosome 1)	GGGAGGAGGAAAGGTGTAG
2000-fwd (chromosome 1)	GCCATAACAGAGGTGGAAG
2000-rev (chromosome 1)	AACCTTAGGATGGGGCTGCT

fwd, forward; rev, reverse.